TECHNICAL REPORT 86-21

Steady-State Flow in a Rock Mass Intersected by Permeable Fracture Zones. Calculations on Case 2 with the GWHRT-code within Level 1 of the HYDROCOIN Project.

Björn Lindbom, KEMAKTA Consultants Co.

Stockholm
December 1986

SVENSK KÄRNBRÄNSLEHANTERING AB
SWEDISH NUCLEAR FUEL AND WASTE MANAGEMENT CO
BOX 5864 S-102 48 STOCKHOLM
TEL 08-65 28 00 TELEX 13108-SKB

STEADY-STATE FLOW IN A ROCK MASS INTERSECTED BY PERMEABLE FRACTURE ZONES

Calculations on case 2 with the GWHRT-code within Level 1 of the HYDROCOIN project

Björn Lindbom
KEMAKTA Consultants Co., Stockholm

December 1986

A list of other reports published in this series during 1986 is attached at the end of this report. Information on KBS technical reports from 1977-1978 (TR 121), 1979 (TR 79-28), 1980 (TR 80-26), 1981 (TR 81-17), 1982 (TR 82-28), 1983 (TR 83-77), 1984 (TR 85-01) and 1985 (TR 85-20) is available through SKB.

PREFACE

An international cooperation project,HYDROCOIN, for studying numerical models for groundwater flow was initiated in May 1984 by the Swedish Nuclear Power Inspectorate (SKI).Fourteen organisations from ten countries are participating in the study.

HYDROCOIN is divided into three levels where Level 1 is devoted to checking the numerical accuracy of the codes used in the study. Formulations of the test cases on which the groundwater flow codes are applied are agreed upon at organised meetings held twice a year thrcughout the three year period the project is planned to last.

This paper describes calculations on Case 2 within Level 1 performed on behalf of the Swedish Nuclear Fuel and Waste Management Co (SKB).

Case 2 is intended to illustrate influences on groundwater flow caused by permeability contrasts and varying levels of discretisation. The geometry of the modelled domain, as well as boundary conditions, are stipulated in the case definition.

The basic calculations according to the case definition include particle tracking and analyses of the distribution of hydraulic head within the domain. In addition to these analyses, consideration is given to the mass conservation in the numerical solution and how it is affected by permeability contrasts and differences in spatial discretisation.

The calculations are performed with the computer code GWHRT which is based on the finite element method.

Stockholm
November,1986

SUMMARY

This report describes calculations within Level 1 of the HYDROCOIN project carried out on behalf of the Swedish Nuclear Fuel and Waste Management Co. (SKB). The simulations are made with GWHRT ,which is a computer code based on the finite element method.

Level 1 of HYDROCOIN consists of seven well-defined test problems. This paper is concerned with Case 2, which is formulated as a generic groundwater flow situation often found in crystalline rock with highly permeable fracture zones in a less permeable rock mass. The case is two-dimensional and modelled with 8-noded, isoparametric, rectangular elements.

According to the case definition, calculations of hydraulic head and particle tracking are to be performed.The computations are carried out with varying degree of discretisation in order to analyse possible impact on the result with respect to nodal density.

Further calculations have been performed in addition to those stipulated in the case specification. They are mainly devoted to mass balance deviations and how these are affected by permeability contrasts, varying degree of spatial discretisation and distortion of finite elements. Totally seven runs have been performed.

According to the results obtained with the GWHRT-code, the distribution of hydraulic head in the domain is less sensitive to differences in nodal density than the trajectories. The hydraulic heads show similar behaviour for three meshes with varying degrees of discretisation.The particle tracking, on the other hand, seems to be more sensitive to the level of discretisation. The results obtained with a coarse and medium mesh indicate completely different solutions for one of the pathlines. The coarse mesh is too sparsely discretised for the specified problem.

The local mass balance is evaluated for seven runs.The mass balance deviation as introduced in this report seems to be considerably more sensitive to the level of discretisation than to both permeability contrasts and deformation of elements. The permeability contrasts between the rock mass and fracture zones vary from a factor of 1000 to 1 (homogeneous properties) with increments of a factor of 10. These calculations in fact give better mass balance with increasing permeability contrasts, contrary to what could be expected. However, these improvements are marginal and cannot be regarded as significant.

A minor deformation of the element mesh is introduced in the last run. The results indicate only small changes in the mass balance deviation.

A general conclusion regarding the behaviour of the GWHRT-code is that it seems to produce results that agree well with other codes that have been applied to this HYDROCOIN test case.

TABLE OF CONTENTS

1 INTRODUCTION

Radioactive waste will most probably be disposed of in the geosphere in the future. The feasibility of the geological formations that might serve as the recipient for such disposal must therefore be investigated. The most likely way for radionuclides to reach human environments from future repositories will be by dissolution and transport in flowing groundwater. These chemical and physical processes need to be understood in this context.

The most common way of making these complex processes comprehensible today is by applying numerical models and simulating the processes with the aid of computer.The results obtained from this kind of study need to be validated against experiments and their numerical accuracy must be verified.

The Swedish Nuclear Power Inspectorate (SKI) initiated an international project called HYDROCOIN in May 1984. This project aims at making intercomparisons between available groundwater flow codes. HYDROCOIN is divided into three levels,the first of which is devoted to verification of the flow codes. The object of Level 2 is validation, whereas Level 3 is concerned with sensitivity analyses.

Level 1 is designed to test the numerical accuracy of independently developed groundwater flow codes. This is done by means of either intercomparing solutions obtained from well defined test cases,or comparing the numerical results with existing analytical solutions.

This paper is concerned with Case 2 within Level 1 of HYDROCOIN. The test problem describes an idealised version of the situation found in fractured crystalline rock, namely high permeability fault zones in a less permeable rock mass with specified topography (3). The purpose is to test the solution convergence with respect to spatial discretisation and capabilities of the different codes to handle permeability contrasts. As analytical solutions have not been available for this problem, the calculations involve a comparison between different numerical solutions.

It is recognised that flow in crystalline rock systems in general is poorly described by two-dimensional models. The main point of this problem, namely the solution convergence with permeability contrasts, will still be appropriately tested in two dimensions.

The results described in this paper were obtained with a code called GWHRT (1). The verification of GWHRT is presented in the report on HYDROCOIN Level 1 (4), where all computational results within Level 1 are compiled and intercompared.

2 HYDROCOIN LEVEL 1 - ASPECTS OF VERIFICATION

The validity of results obtained with numerical simulations needs to be tested and the computer code has to be verified. A true verification can be performed only if analytical solutions exist with which the results can be compared. However,analytical solutions are available only for simplified cases. Verification of the codes therefore often has to be carried out by means of intercomparisons between results from different simulations of a specified problem. If results that are obtained with independently developed codes appear to agree within acceptable limits, the codes in question can be considered verified.

The test cases included in Level 1 of HYDROCOIN are thoroughly defined,which implies that the prerequisities are unambiguous with respect to boundary conditions,hydraulic properties etc.

Nevertheless, the codes that are used in the study differ somewhat from each other; some are based on the finite difference technique while others use the finite element method. Moreover,the type of finite elements can differ from code to code.

HYDROCOIN project meetings are organised twice a year when the participants discuss formulations of test problems and present their results. The results are discussed and intercomparisons are made between the codes that are used to simulate each case. These meetings have proved to be a valuable forum for exchanging ideas and drawing conclusions. During these sessions is it possible to compare a high enough number of different sets of results to be able to claim that the codes are verified.

A presentation of Case 2 results obtained with the GWHRT-code has been given at one of the meetings. There appears to be a high degree of resolution with the results obtained using other codes, which means that GWHRT can be considered verified in this context.

Complete textual and pictorial intercomparisons regarding the results within Level 1 of HYDROCOIN are described in detail in a separate report (4).

3 BRIEF DESCRIPTION OF GWHRT COMPUTER CODE

GWHRT is a computer code developed by Roger Thunvik et al (1) to simulate coupled heat and groundwater flow. It is a model with the continuum approach based on the Galerkin formulation of the finite element method in either two or three dimensions.

The model consists of coupled non-linear partial differential equations for heat and groundwater flow through fractured rock. The governing equations are solved numerically and transformed into a set of algebraic equations which are solved by Gaussian elimination using the frontal method.

The finite elements used in this case are isoparametric, two-dimensional, quadri-lateral elements with eight nodal points.In three dimensions brick elements with 20 nodal points are used. The interpolation is quadratic in both of these types of elements.

In addition to this FEM-model, several other programs are used to pre- and post-process the finite element meshes. These programs are for example designed to optimise the mesh with respect to the band- and front-width, calculating isopotentials, tracking particles, checking mass balance etc. They are all included in a program package called HYPAC for the pre- and post-processing of finite element data and are the subject of a separate report (2).

GWHRT is implemented on an Amdahl-470 at Stockholm University Computing Center. All the calculations referred to in this report are computed on this machine.

4 SPECIFICATION OF THE TEST PROBLEM

4.1 Conceptual Model

A two-dimensional cross-section of a fractured rock is intersected by two fracture zones (see Figure 1). The zones are inclined so that they intersect at some depth. The topography has been simplified so that it consists of two valleys in which the fracture zones come up to the surface. The slopes are described as straight lines. The widths, as well as the inclinations, of the fracture zones are different, which means that the flow pattern is expected to be asymmetric despite the symmetric topography. Steady state and isothermal conditions are assumed.

It is assumed that Darcy's law is applicable both for the fracture zones and for the rock matrix around the zones. The matrix and the fracture zones are regarded as two homogeneous and isotropic media.

4.2 Mathematical Model and Boundary Conditions

As this is a steady state problem, both the flow in the matrix and in the fracture zones can be described by the Laplace equation:

$$\nabla^2 h_m = 0 \qquad (1)$$

$$\nabla^2 h_f = 0 \qquad (2)$$

where $h_m = h_f$ at the interface between matrix and fractures, ∇ is the gradient operator, h_m and h_f are the hydraulic heads in the matrix and the fracture zone respectively.

The boundary conditions for the top surface (ground surface) are:

$$h_m = h_f = z \qquad (3)$$

where z is the vertical space coordinate.

Non-flow conditions are assumed at the vertical boundaries:

$$\left.\frac{\partial h_m}{\partial x}\right|_{\substack{x=0 \\ x=1600}} = 0 \qquad (4)$$

where x is the horizontal space coordinate.

The bottom boundary (z = -1000 m) is also assumed to be impervious, i.e.:

$$\left.\frac{\partial h_m}{\partial z}\right|_{z=-1000} = \left.\frac{\partial h_f}{\partial z}\right|_{z=-1000} = 0 \qquad (5)$$

Equations (1)-(5) imply that the only driving force on the groundwater flow is the sloping topography. The boundary conditions are indicated in Figure 1.

5 VARIATIONS OF INPUT PARAMETERS

According to the case definition (3) a series of at least two calculations is to be performed with different levels of spatial discretisation. In this particular exercise three levels of discretisation have been used.

Within this project certain additional calculations, mainly devoted to the massconservation of the numerical solutions and how these are affected by permeability contrasts and varying nodal density, are performed.

A total of seven runs have been performed,which differ with respect to either hydraulic conductivity or spatial discretisation. These runs are from now on referred to as Cases 1-7.

All the calculations are performed with 8-noded,isoparametric, quadri-lateral finite elements in two dimensions.

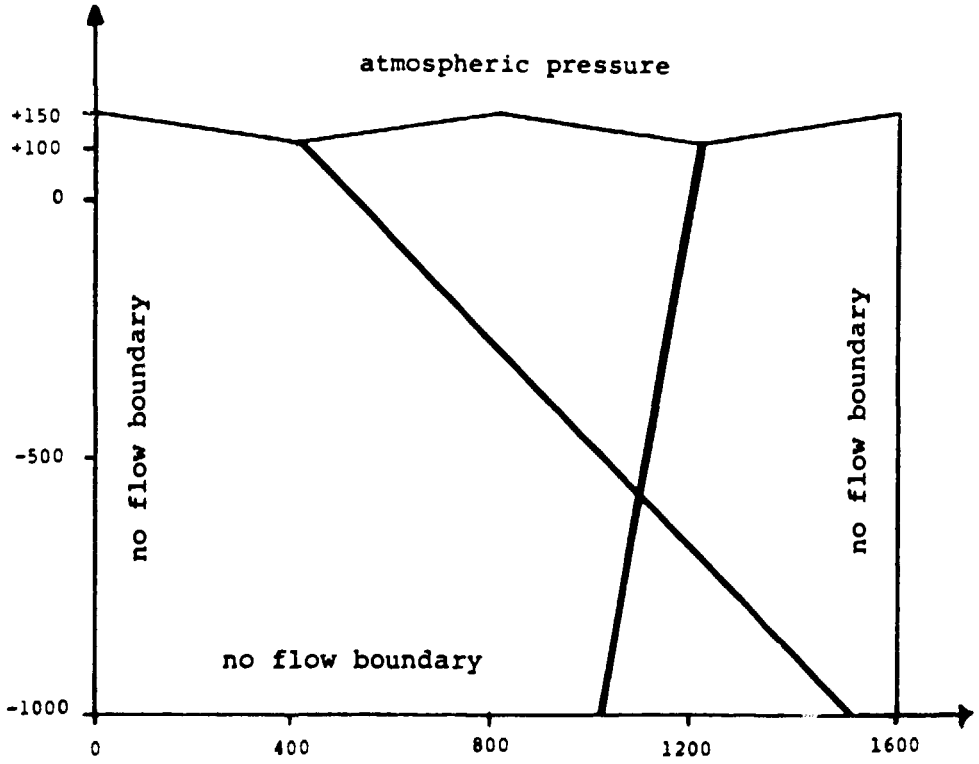

Fig. 1 Geometry of the modelled domain with boundary conditions indicated.

Cases 1-3 are simulated in agreement with the case definition with constant hydraulic properties, whereas they differ internally in terms of the level of discretisation. Cases 4-6 use the same spatial discretisation as Case 3 but the permeability contrast between the matrix and fracture varies between a factor of 1000 and no contrast at all.

The last run, Case 7,is calculated with the same hydraulic properties as assigned to Case 3. Even the numbers of nodal points and finite elements are the same as for Case 3, whereas the mesh is rearranged somewhat in order to be able to study the effect of element distortion.

The hydraulic properties and the number of nodal points and elements are shown in Table 1.

Table 1. Hydraulic properties and number of nodal points for each case.

Case no.	Hydr.cond. m/s matrix	Hydr. cond. m/s fractures	No. of nodes	No. of elements
1	$1 \cdot 10^{-8}$	$1 \cdot 10^{-6}$	190	53
2	$1 \cdot 10^{-8}$	$1 \cdot 10^{-6}$	504	151
3	$1 \cdot 10^{-8}$	$1 \cdot 10^{-6}$	1582	497
4	$1 \cdot 10^{-8}$	$1 \cdot 10^{-8}$	1582	497
5	$1 \cdot 10^{-8}$	$1 \cdot 10^{-7}$	1582	497
6	$1 \cdot 10^{-8}$	$1 \cdot 10^{-5}$	1582	497
7	$1 \cdot 10^{-8}$	$1 \cdot 10^{-6}$	1582	497

The hydraulic conductivities are assigned element-wise. Isotropic and homogeneous conditions are assumed.

A porosity of 0.03 was maintained throughout all of the seven cases.

The four meshes are shown in Figures 2a-d. Figure 2e is intended to show the difference between the meshes used for Cases 3 and 7.

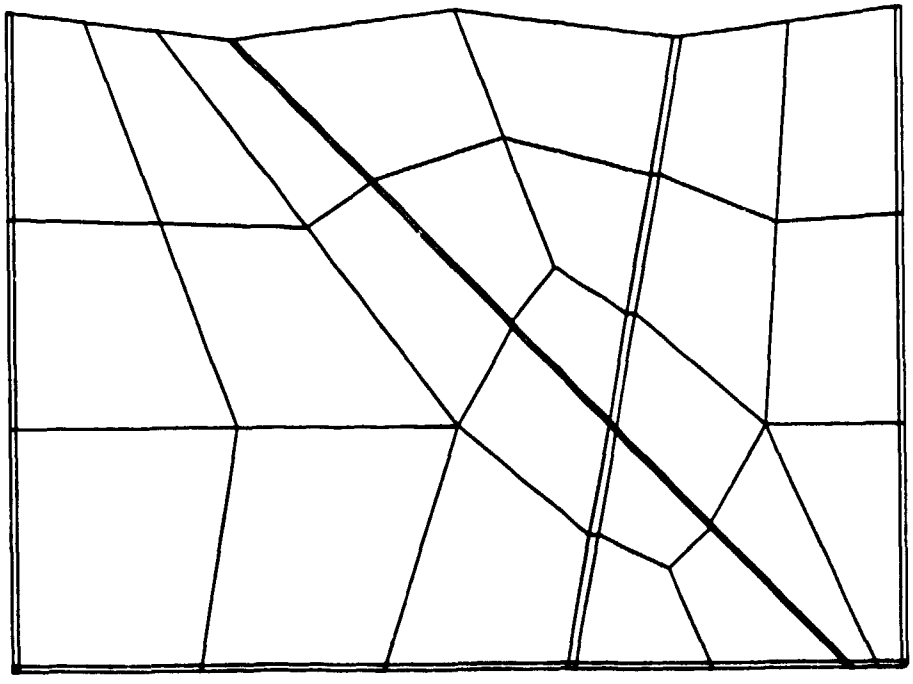

Fig. 2a Coarse mesh used for Case 1.

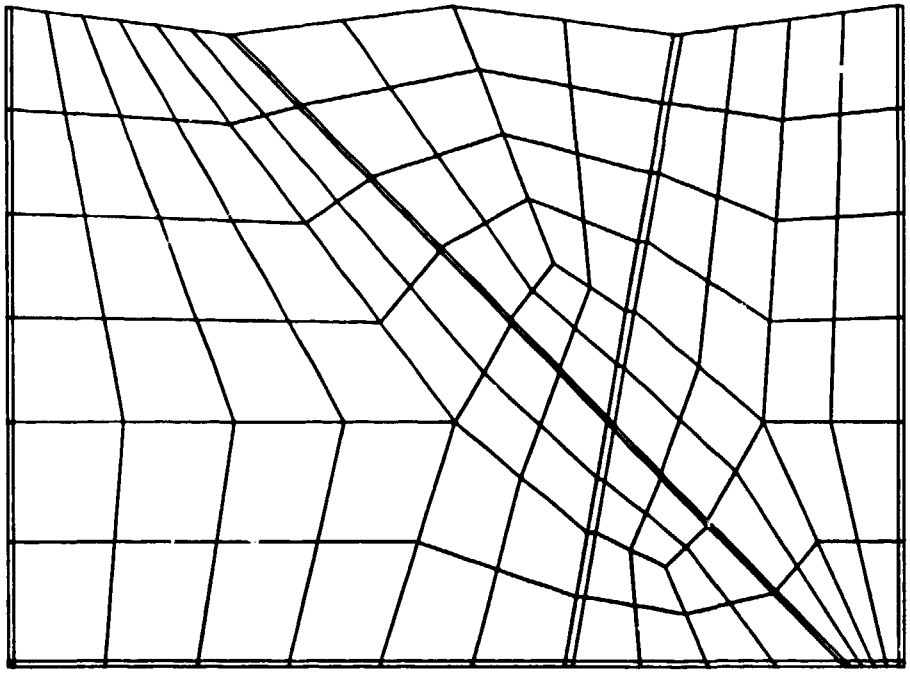

Fig. 2b Medium mesh used for Case 2.

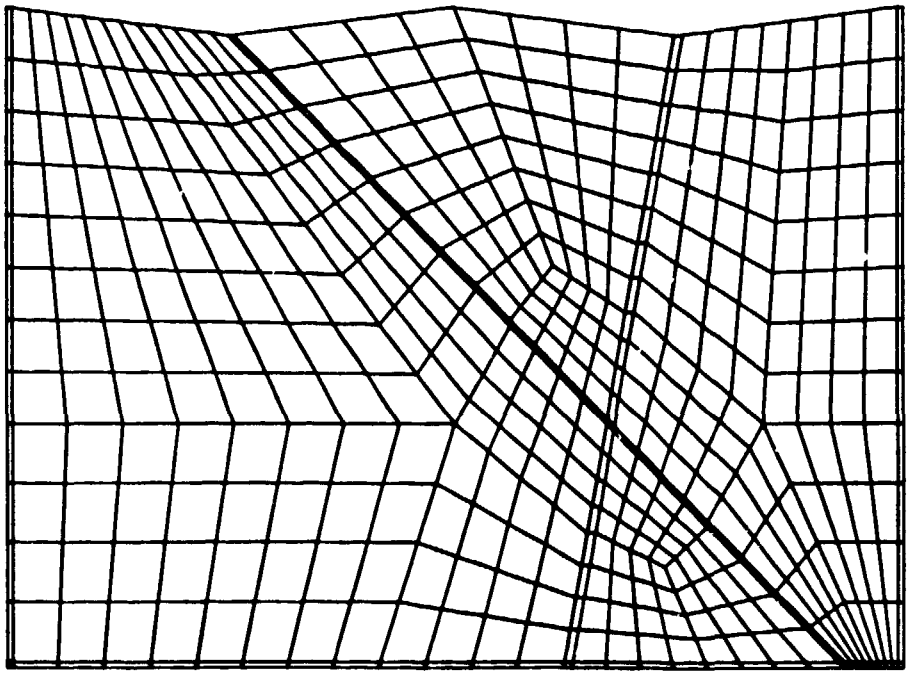

Fig. 2c Fine mesh used for Cases 3,4,5 and 6.

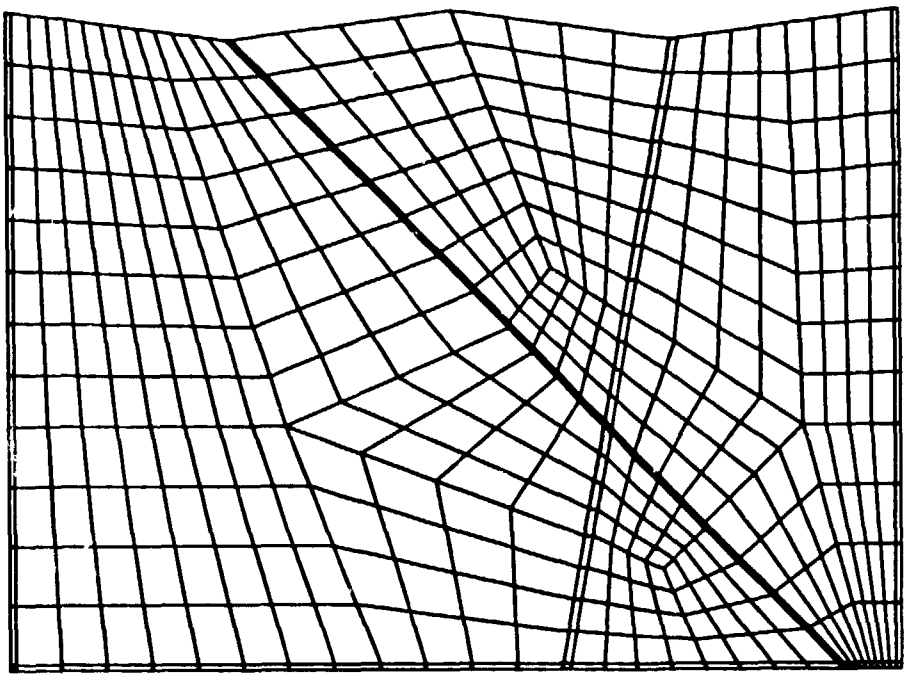

Fig. 2d Fine mesh rearranged used for Case 7.

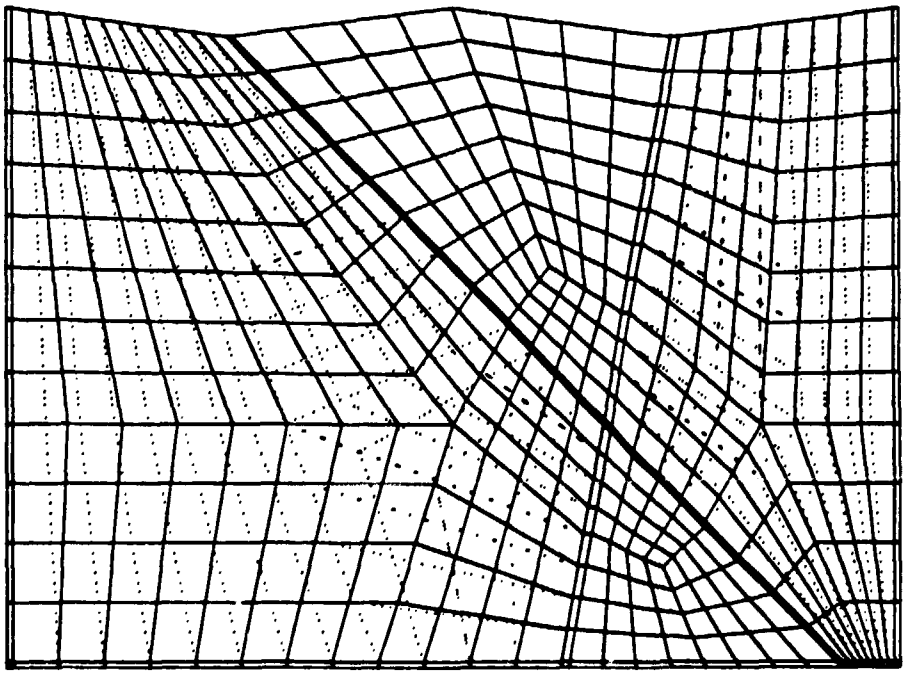

Fig. 2e Fine mesh used for Case 3,4,5 and 6 (solid)
and rearranged fine mesh used for Case 7 (dotted).

6 REQUIRED OUTPUT

6.1 Output According to Case Definition

The required output according to the specification of the test case is the distribution of hydraulic head along five horizontal lines through the modelled domain. The lines are located at: z= 0, - 200, -400, -600 and -800 (metres).

In addition, tracking of 4 trajectories is to be performed. The starting positions for these are as follows:

Trajectory no. 1 x = 100; z = 0
Trajectory no. 2 x = 100; z = -200
Trajectory no. 3 x = 1500; z = 0
Trajectory no. 4 x = 1500; z = -450

The horizontal lines along which the hydraulic head is to be calculated are depicted together with the starting positions for the trajectories in Figure 3 . These types of calculations are only performed for Cases 1-3 in this study.

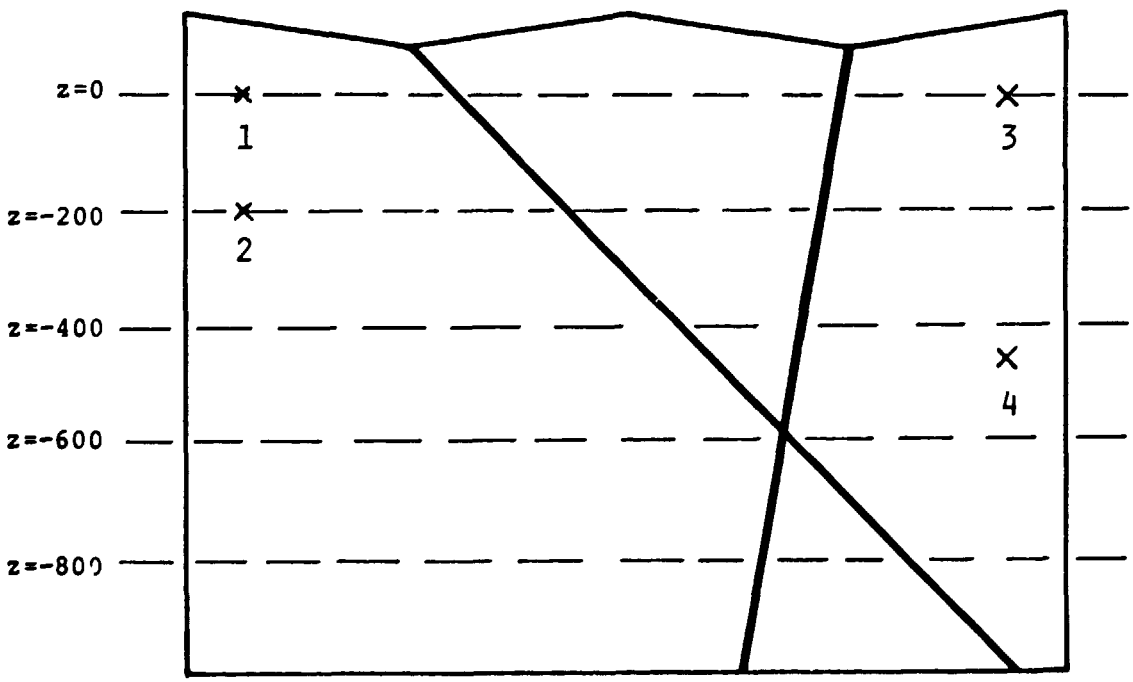

Fig. 3 Five horizontal lines along which the hydraulic head is to be calculated. The four points indicate starting positions for trajectories 1-4 resp.

6.2 Output from Additional Calculations

The main objectives of the additional calculations are to analyse the local mass conservation in the numerical solutions and how it is affected by permeability contrasts and differences in spatial discretisation. For this purpose, element-wise mass balance deviations are calculated for all the cases, including Cases 1-3.

Apart from this type of calculation, flow vectors and isopotential curves are computed and plotted for Cases 1-7.

A description of how the mass balance deviation is calculated is given in Section 7.2 .

7 CALCULATIONS PERFORMED

7.1 Head Distribution and Particle Tracking

The calculations of head distribution along specified lines and particle tracking are run with three levels of discretisation (Cases 1-3). These meshes are shown in Figures 2a-c and the number of nodal points and elements are indicated in Table 1 (see Chapter 5).

As was requested in the definition of the test problem, the distribution of hydraulic heads is calculated along five horizontal observation lines; located at depths of $z = 0$, $z = -200$, $z = -400$, $z = -600$ and $z = -800$. These observation lines cross the entire domain. The head is calculated at some 100 points along each line where the value is interpolated from nodal values using the element shape functions.

Four pathlines are tracked, the starting positions of which are located rather close to the two vertical boundaries in order to see if the tracking algorithm is capable of handling the permeability contrasts occurring in the domain.The particles are tracked with an Eulerian stepping algorithm (explicit or forward differencing).

Flow vectors and isopotential curves are calculated for Cases 1-7. The flow vectors originate from the centre of the element and are logarithmically scaled by one vector per element. The isopotential curves are plotted in the same frame as the flow vectors.

7.2 Mass Balance Deviation

The impact of the following parameters is analysed within this study:

- level of discretisation (Cases 1-3)
- permeability contrast (Cases 4-6)
- distortion of the finite elements (Case 7)

By estimating the local mass balance it is possible to measure the quality of the numerical solution. This is done here by stating a mass conservation deviation index, D_e, related to the flow into and out of each element according to the formula below:

$$D_e = \frac{\Sigma i_n}{\Sigma |i_n|}$$

where i_n corresponds to the flow into or out of one element through the n faces of the element. Inflow is regarded as negative and outflow consequently as positive. An element with a completely conservative solution will have a deviation index equal to zero with this notation, whereas a deviation index of 100% will correspond to a flow either only into or out of the element.

Plots of the meshes are presented where the elements have been filled with different fill-patterns corresponding to the deviation indices.

8 RESULTS

8.1 Head Distribution

The distribution of hydraulic head along the five observation lines is depicted in Figures 4-8. All figures indicate the same tendency of the fractures to drain the water by less steep gradients with increasing depths. The draining influence of the fracture that dips least also decreases with depth. Figure 5 shows a tendency to the effect that water at this depth leaves the domain through the steeper fracture, but is introduced from the middle part of the other one. This tendency is emphazised in Figures 7 and 8.

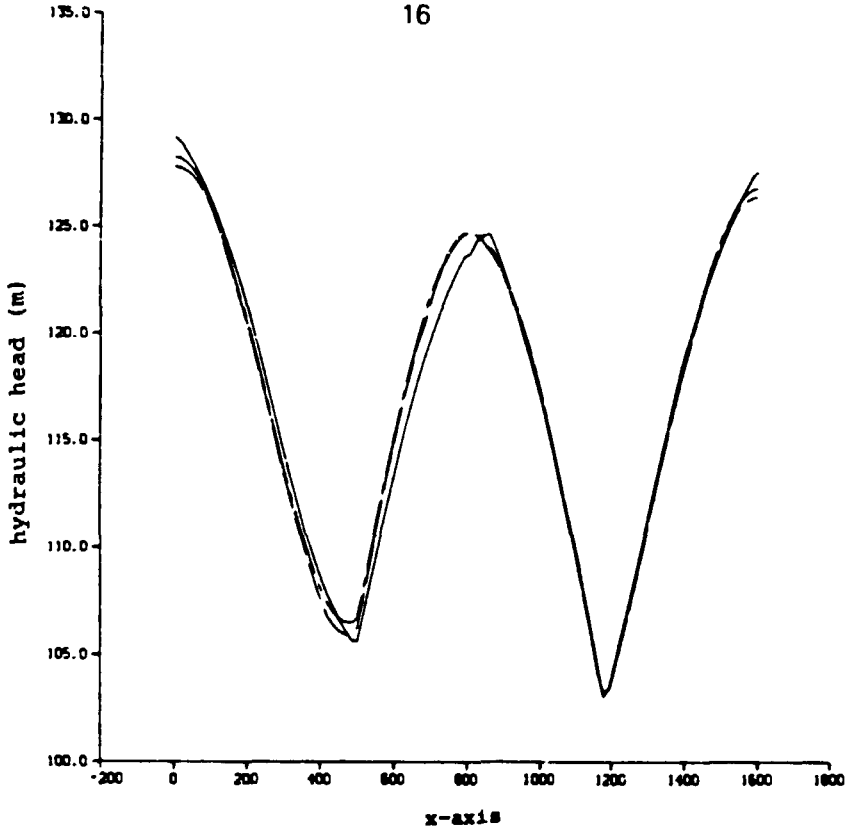

Fig. 4 Distribution of hydraulic head at z=0; solid line - Case 1, dashed line - Case 2, chain dashed line - Case 3.

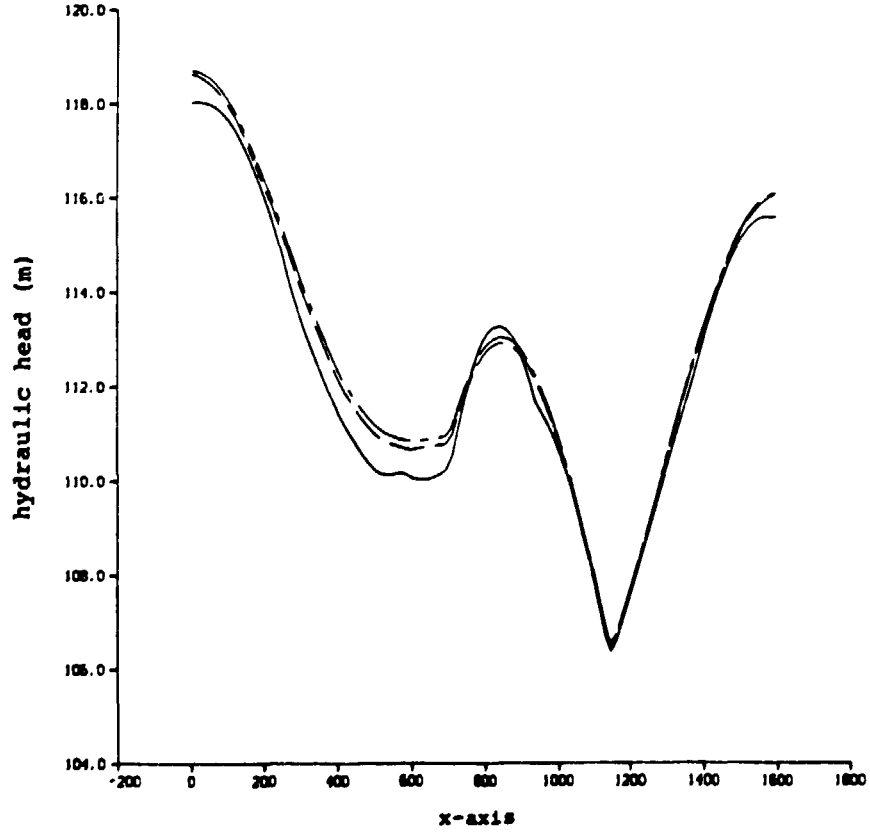

Fig. 5 Distribution of hydraulic head at z=-200; solid line - Case 1, dashed line - Case 2, chain dashed line - Case 3.

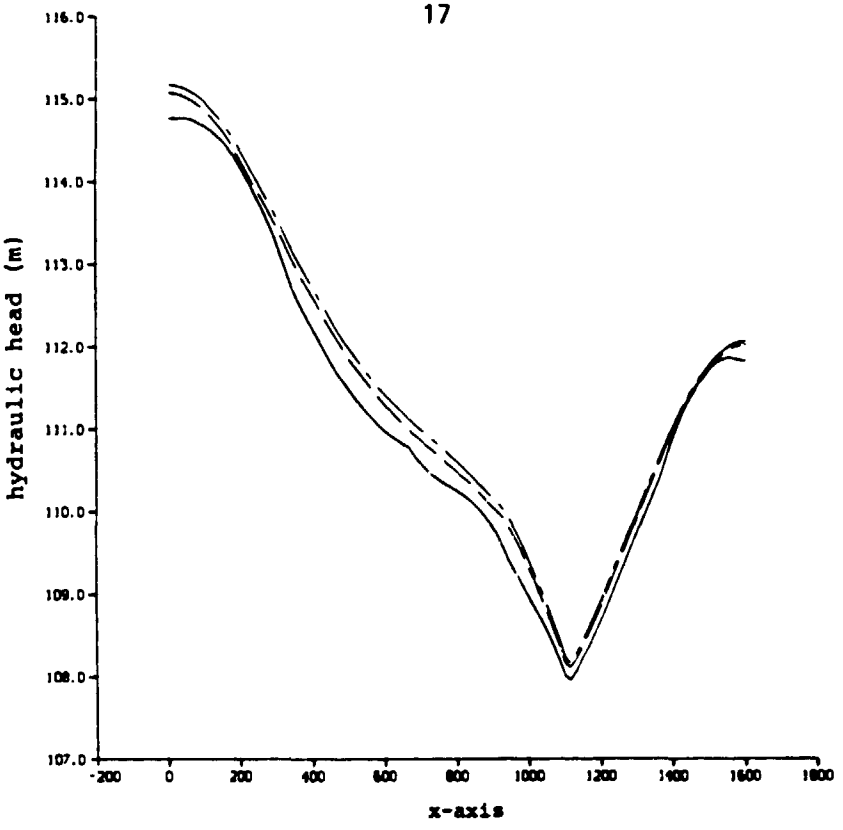

Fig. 6 Distribution of hydraulic head at z=-400; solid line - Case 1, dashed line - Case 2, chain dashed line - Case 3.

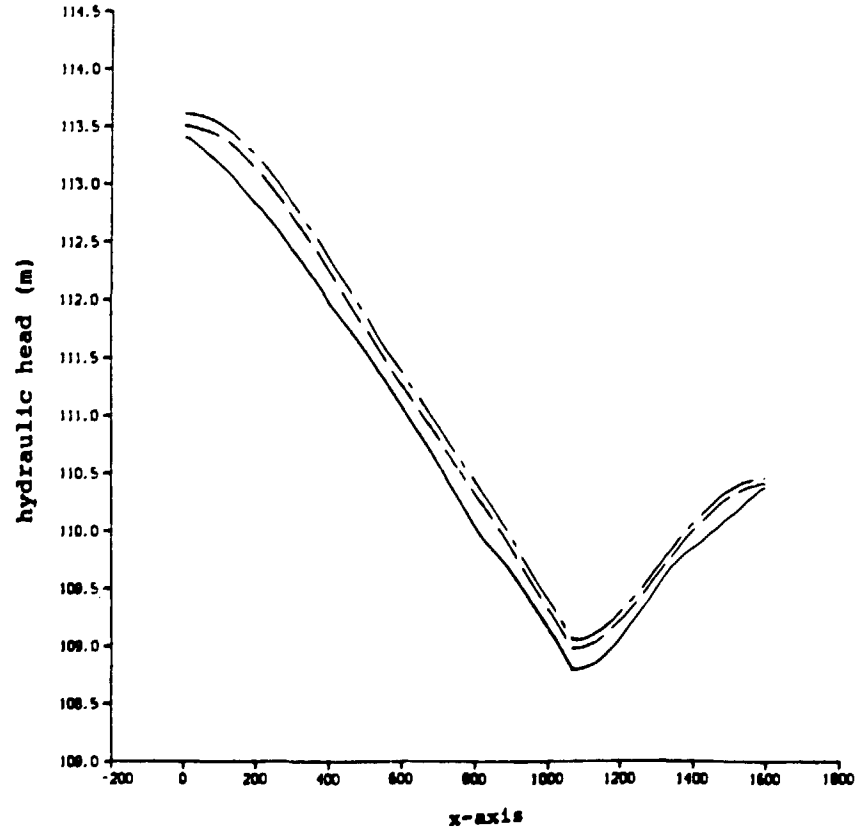

Fig. 7 Distribution of hydraulic head at z=-600; solid line - Case 1, dashed line - Case 2, chain dashed line - Case 3.

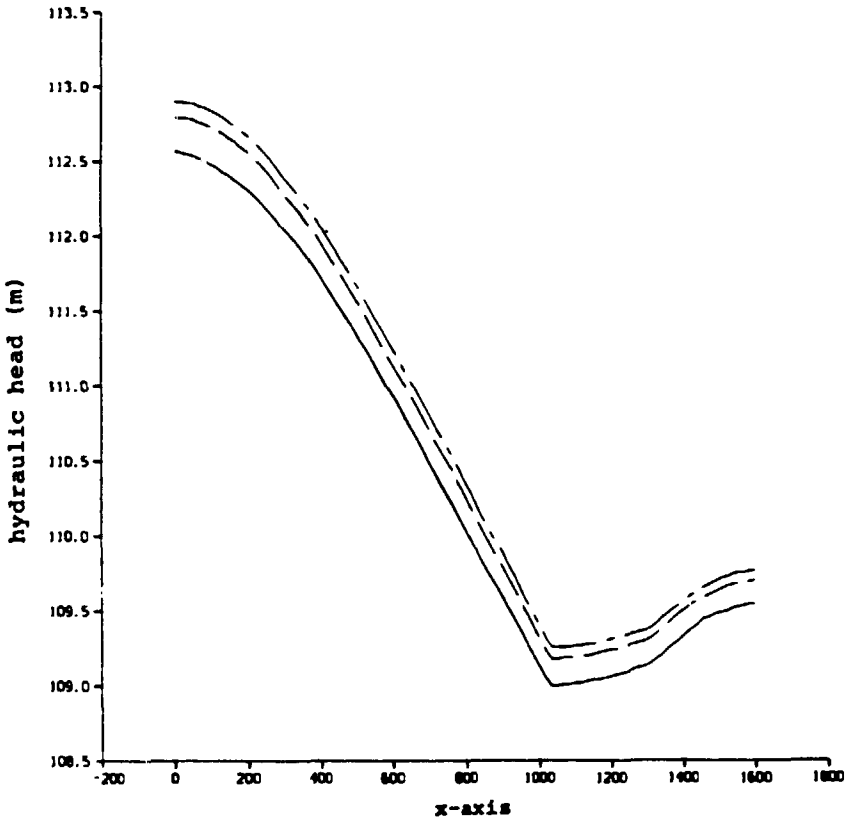

Fig. 8 Distribution of hydraulic head at z=-800; solid line - Case 1, dashed line - Case 2, chain dashed line - Case 3.

The coarse mesh generally produces lower values than the finer ones on the hydraulic head, regardless of the spatial location. This impression is emphazised with increasing depth and the discrepancy between the levels of discretisation grows with depth.

The gap between the values obtained with the coarse mesh and those obtained with the medium mesh is greater than the corresponding difference between the medium and fine meshes. This indicates that a further refinement would imply an even smaller gap between the fine and an even finer mesh.

8.2 Particle Tracking

Regardless of the nodal density, it is obvious that the results for the three meshes show similar solutions for Pathlines 1, 3 and 4, see Figures 9-11.

However, Pathline 2 for Case 1 shows a solution that is completely different from the solutions obtained with the two finer meshes. The magnitude of the gradient on the level of Z= -200 is of about the same order for the three meshes. This means that the total flow in this region is in the same range, but in the coarse mesh the flow is directed horizontally towards the fracture.

The flow in the two finer meshes shows a slightly sub-horizontal direction towards the intersection between the two fractures. The discretisation in the coarse mesh is too sparse for the solution algorithm to find the water divide in this particular region.

Moreover, particle number 4 is 'trapped' in the element describing the fracture intersection when the coarse mesh is used,further reflecting the sparse discretisation in Case 1, see Figure 9.

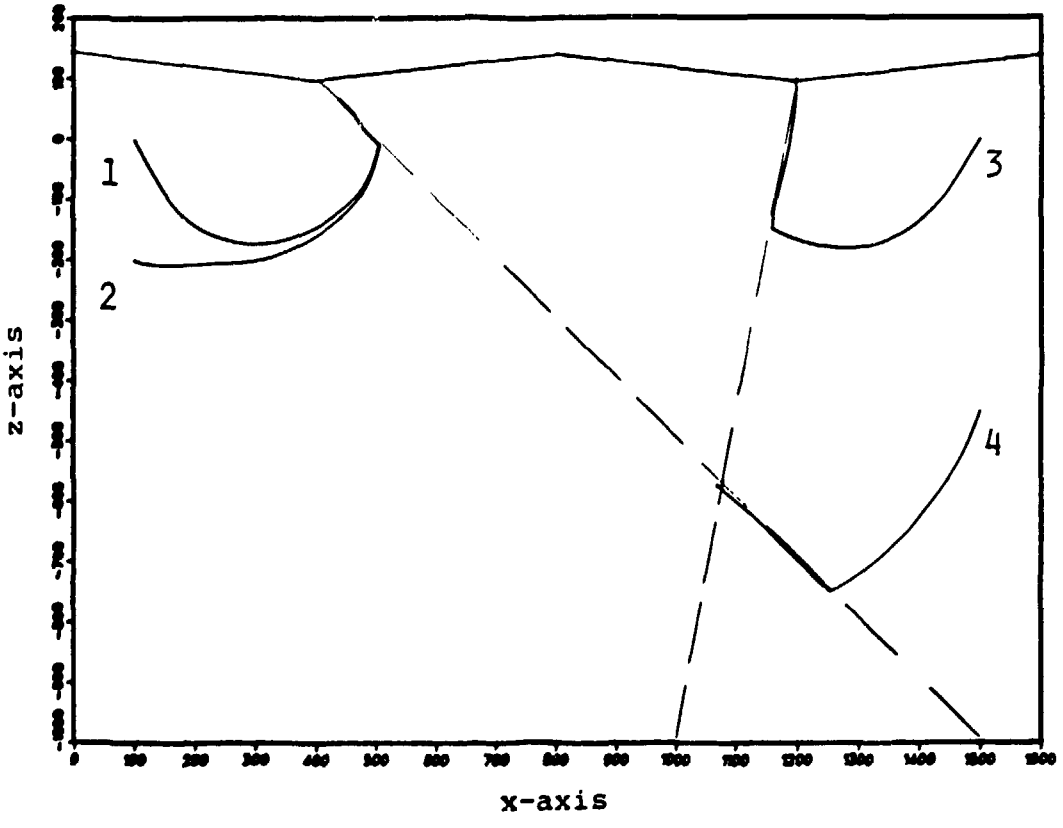

Fig. 9 Pathlines 1-4 using the coarse mesh, Case 1.

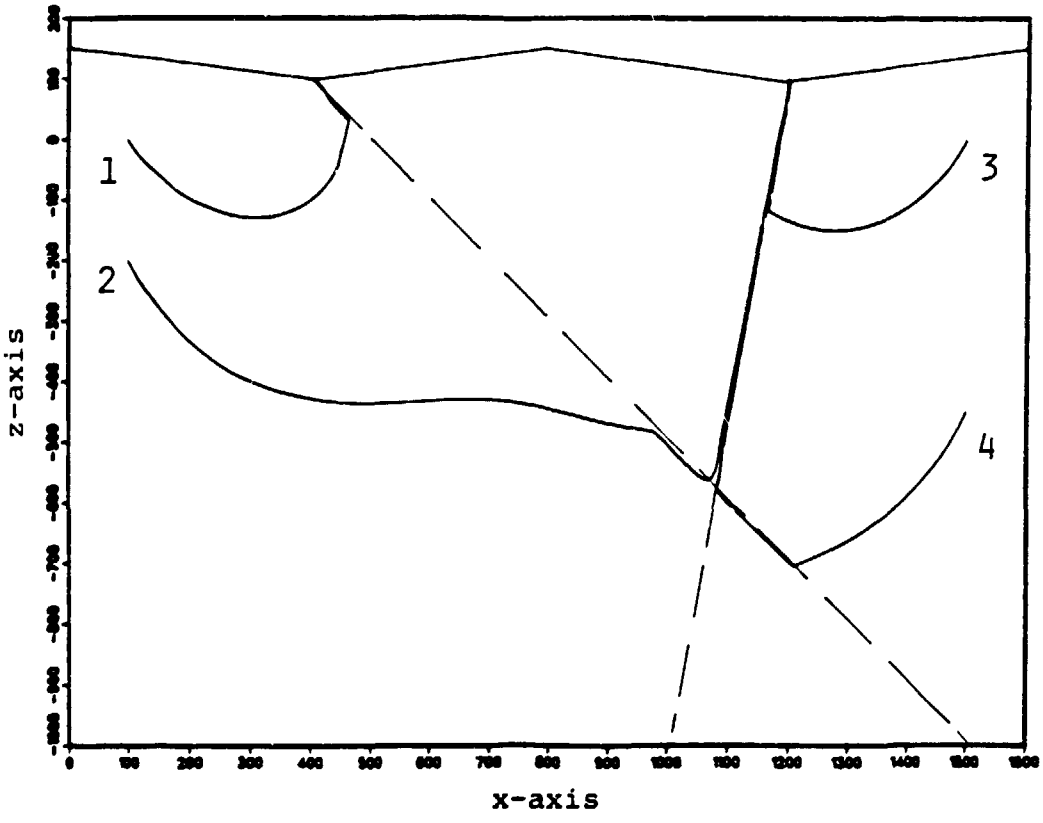

Fig. 10 Pathlines 1-4 using the medium grid, Case 2.

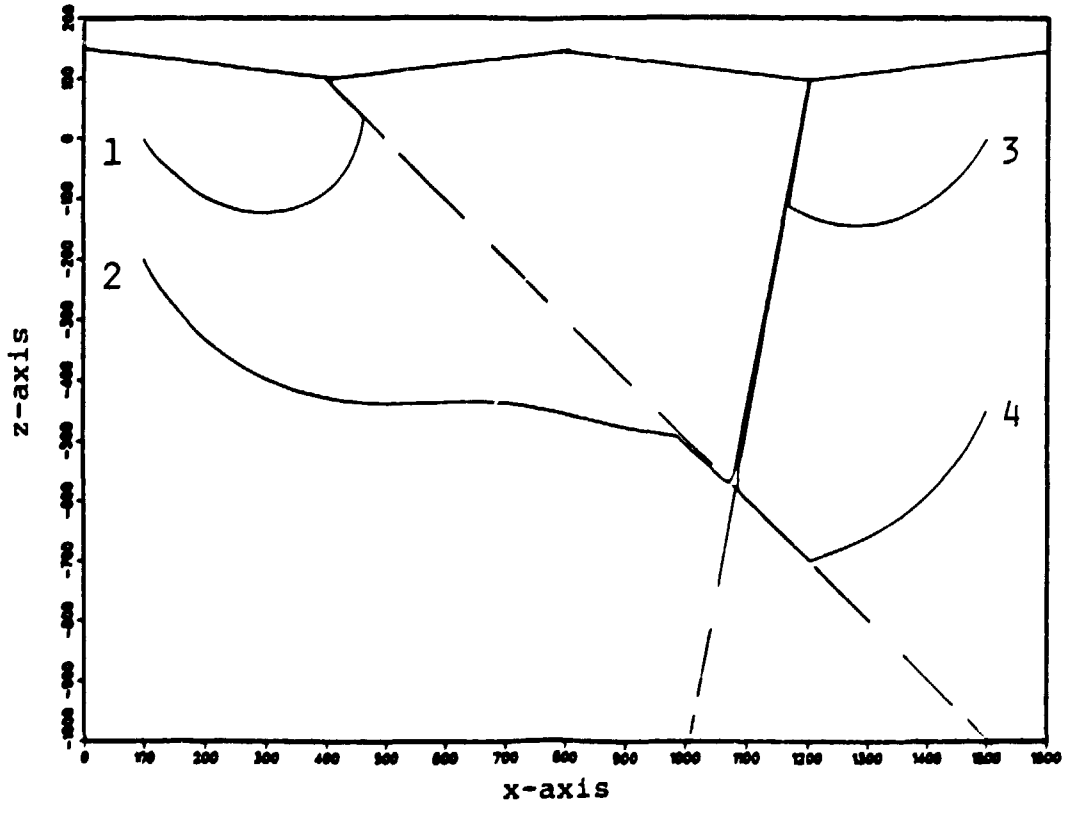

Fig. 11 Pathlines 1-4 using the fine grid, Case 3.

8.3 Mass Balance Deviation

8.3.1 Level of Discretisation (Cases 1-3)

This stage comprises three steps of refinement of the finite element mesh, and the impact of increased discretisation is studied. The hydraulic properties are kept constant according to Table 1 (see Chapter 5).

The finite element meshes for these three cases are shown in Figure 2a-c. The thin rows of elements running along the bottom and vertical boundaries are modelled merely to minimize the numerical disturbances at the borders.

- Coarse mesh, Case 1

  This mesh consists of 53 finite elements and 190 nodal points, see Figure 2a (Chapter 5). Owing to the low number of elements, and hence the expected poor solution, the flow in Figure 13 is significantly discontinuous at the element interfaces,as indicated by the sharp bends on the isobars.

  The chart showing the mass balance deviation index indicates large areas with considerable deviations. This is evident in the lower right-hand corner with an area indicating a deviation exceeding 50%,see Figure 12.

  Almost the entire part of the domain located above the intersection between the fractures reveals a poor numerical solution of the flow field and hence a mass balance deviation index of between 20% and 50%.

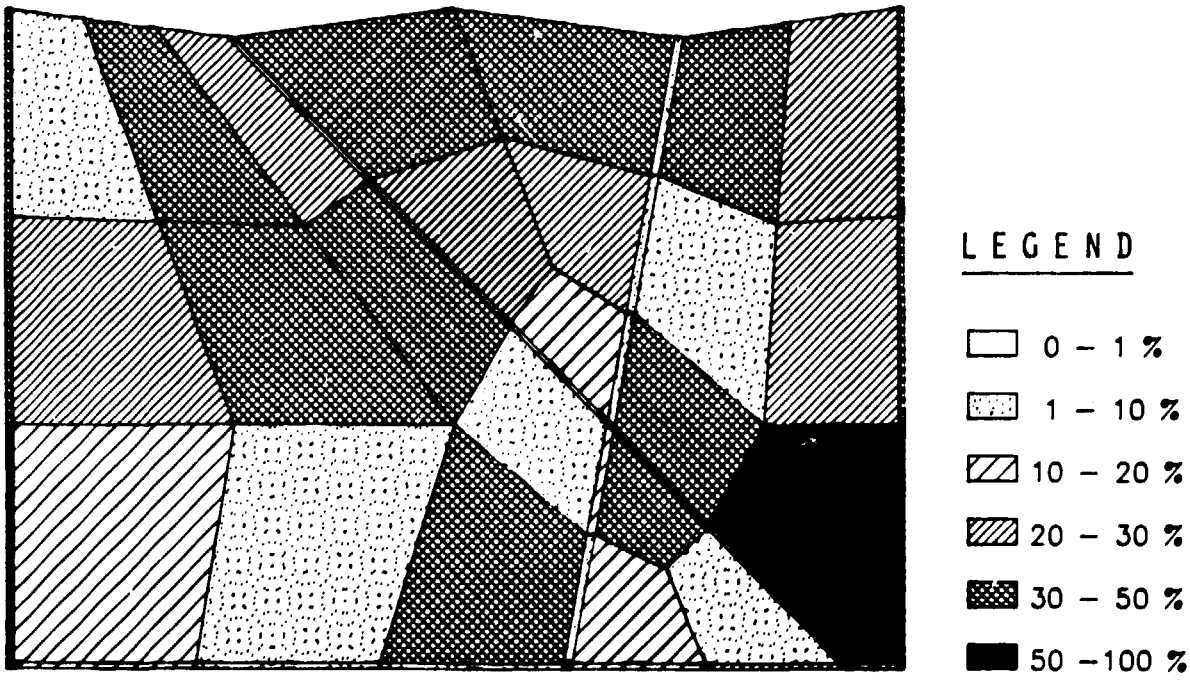

Fig. 12 Mass balance deviation index in Case 1.

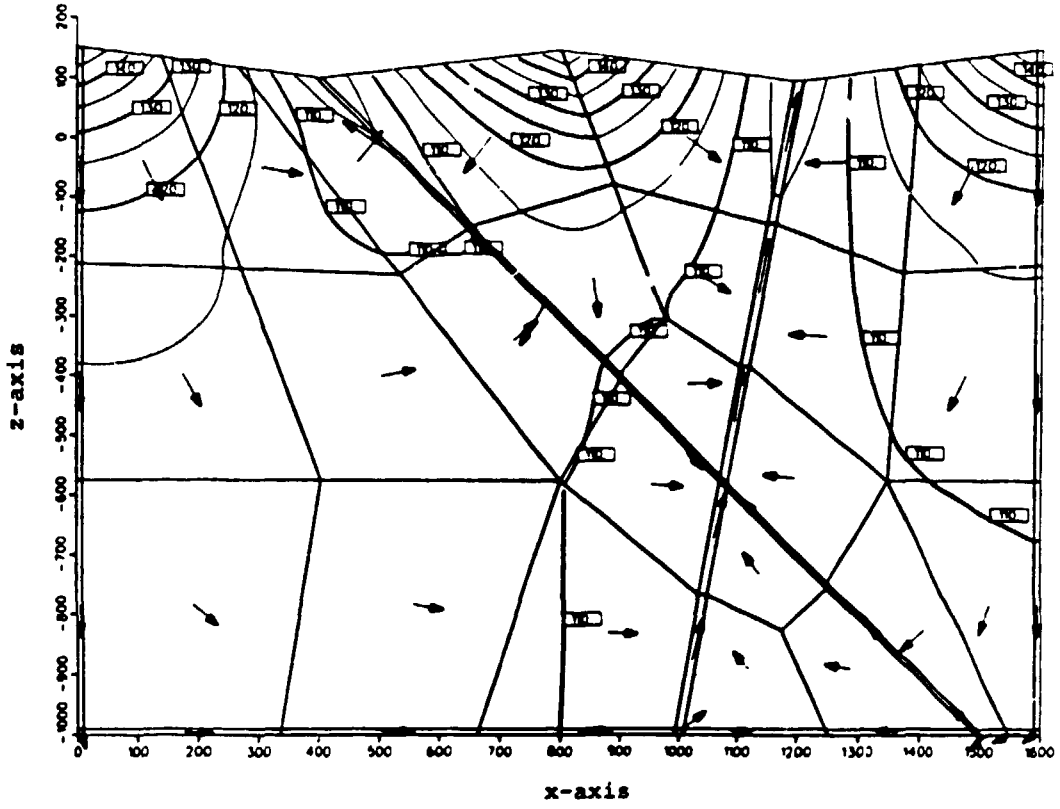

Fig. 13 Isopotentials and flow vectors in Case 1.

- Medium mesh, Case 2

  The number of elements is here increased to 151 with a total number of 504 nodal points, see Figure 2b (Chapter 5).

  The refinement of the mesh gives a lower deviation index compared to Case 1, see Figure 14. The region in the lower right-hand corner indicates that the solution has improved although it still is rather poor. The deviation index is here in the range of 20-50%.

  The numerical solution for the upper half of the domain has also improved; generally a deviation index of about 10-20% is prevalent in this area.

  Moreover, the isobars are smoother than for Case 1 (compare Figures 13 and 15) indicating a higher degree of continuity in the gradient.

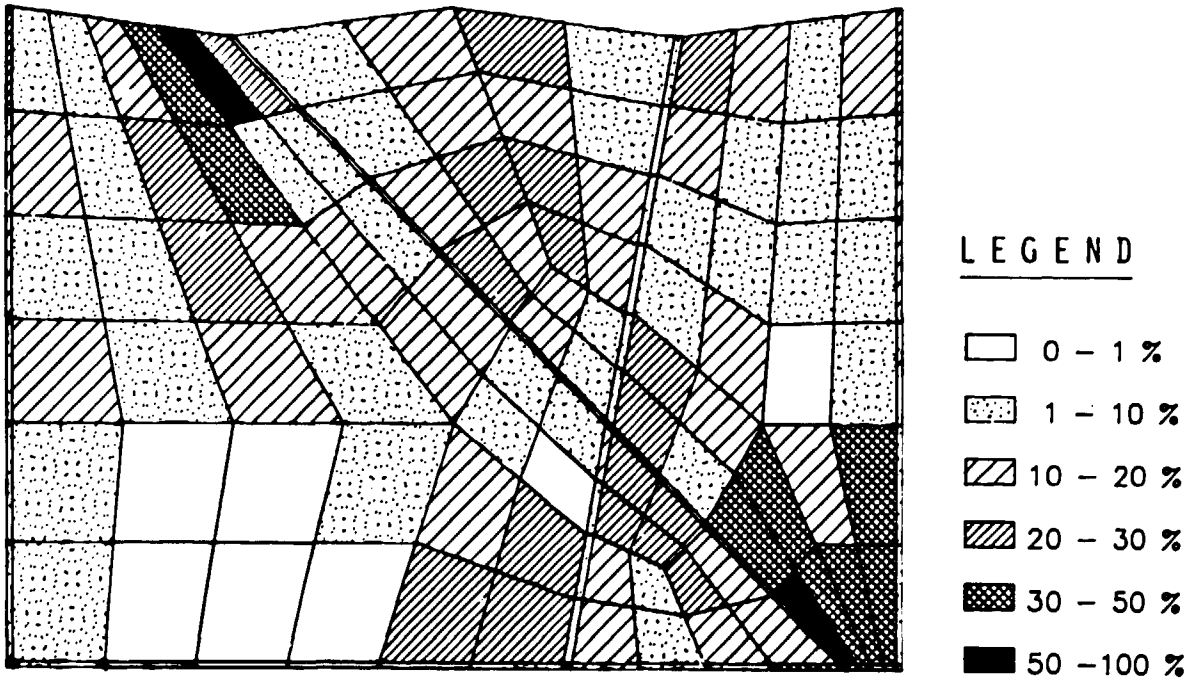

Fig. 14 Mass balance deviation index in Case 2.

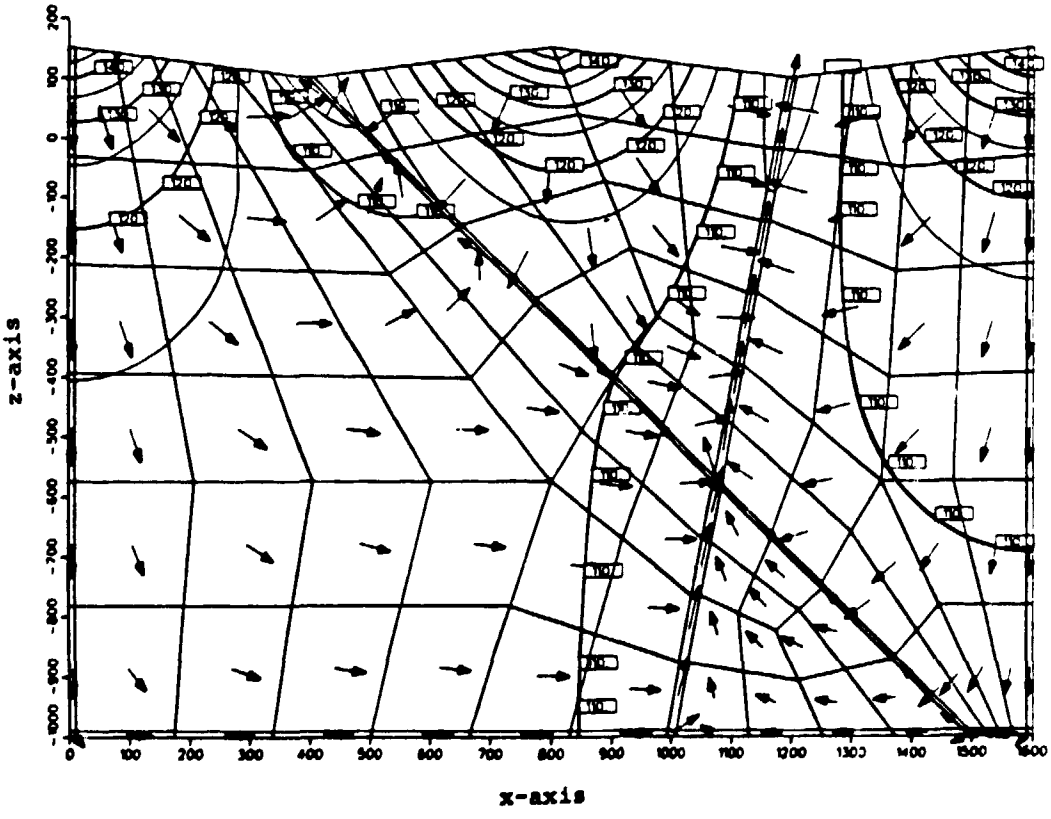

Fig. 15 Isopotentials and flow vectors in Case 2.

- Fine mesh, Case 3

The fine mesh consists of 497 elements with 1582 nodal points as shown in Figure 2c (Chapter 5). This further refinement of the mesh should lead to a mass balance deviation superior to the previous two cases, which also becomes obvious from comparing Figure 16 with Figures 12 and 14. A rather large area in the lower left part of the domain represents a mass balance deviation of less than 1%. This 1%-pattern is elsewhere indicated spot-wise unevenly distributed over the entire domain.

The solution for the region in the lower right-hand part has further improved, as has that of the upper region between the fractures.

The flow vectors and isobars in Figure 17 deviate only slightly from those of Case 2 (Figure 15). The fracture zones evidently drain the system, the wider fracture moreso than the thinner one.

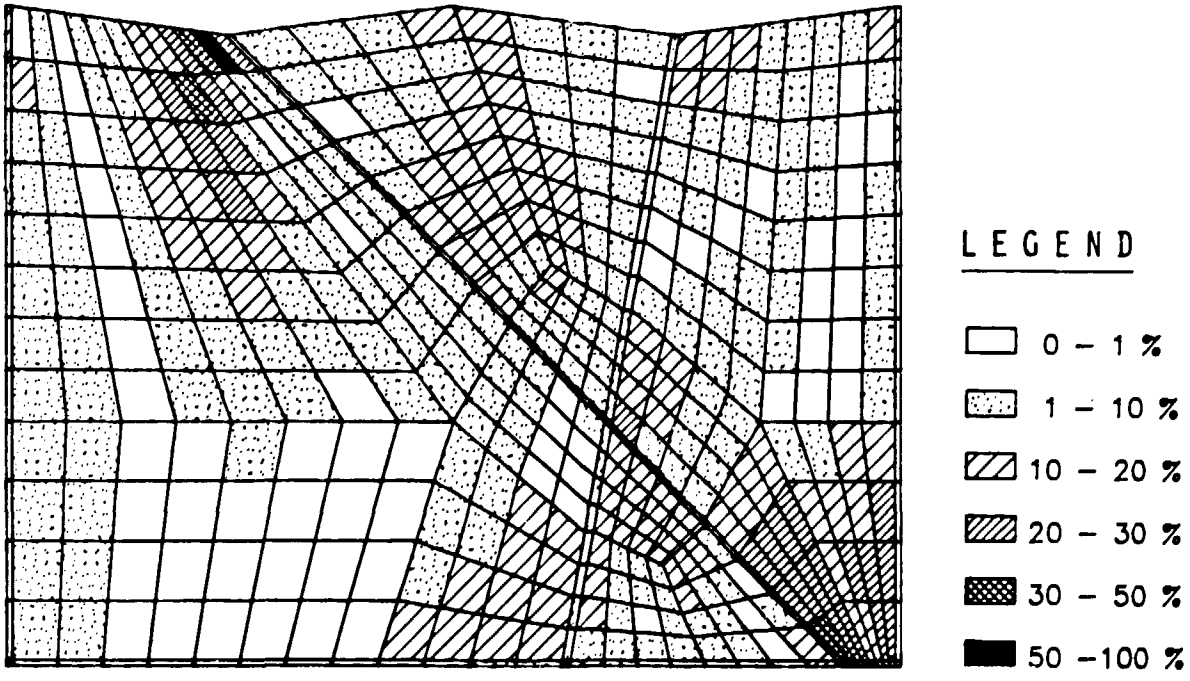

Fig. 16 Mass balance deviation index in Case 3.

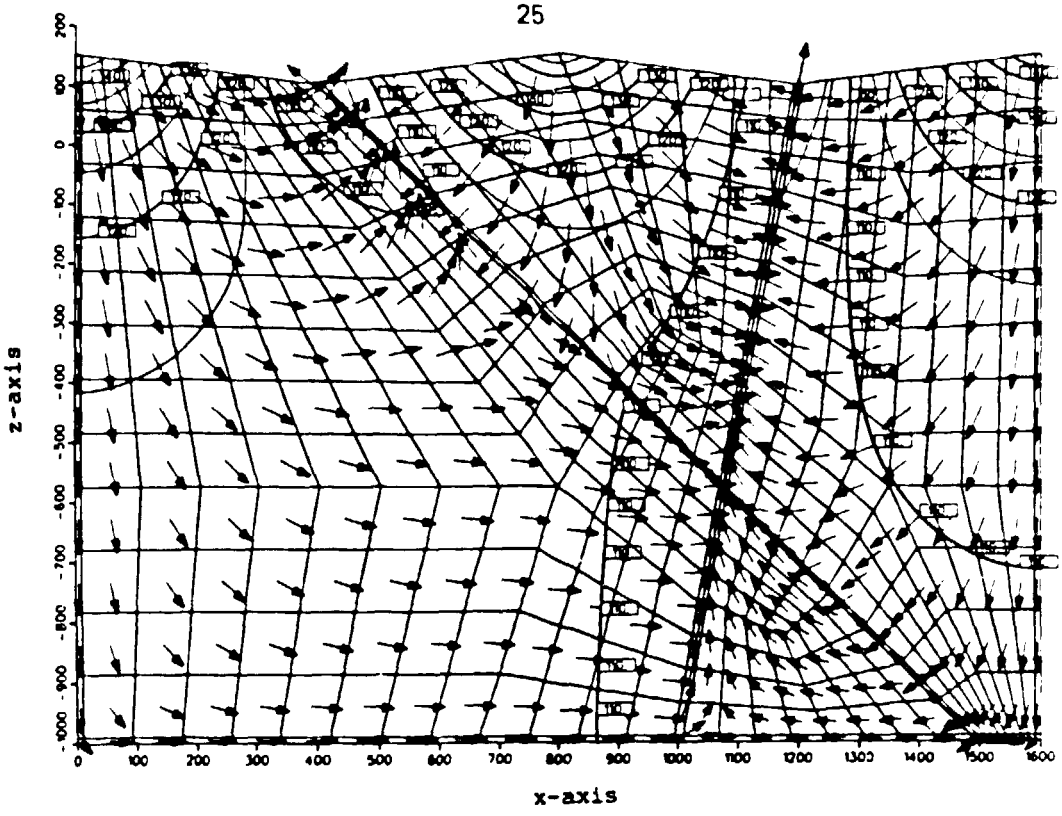

Fig. 17 Isopotentials and flow vectors in Case 3.

8.3.2 Permeability Contrast (Cases 4-6)

This part of the study is mainly intended for illustrating mass balance deviations caused by varying degrees of contrasts in hydraulic conductivities between the rock matrix and the fracture zones.

For this purpose, the finest mesh (used for Case 3) is used as a "base-grid", see Figure 2c (Chapter 5). The hydraulic conductivities are assigned according to Table 1 (Chapter 5) by stepwise increases in the contrast between the rock mass and the fractures.

- Homogeneous hydraulic conductivity, Case 4.

  This case is used as a reference case and is characterized by the hydraulic conductivity being the same throughout the entire domain. From Figure 19 this homogeneity is clear; the flow pattern is close to symmetrical with respect to two vertical lines X= 400 and X=1200, corresponding to the two valleys on the top surface. The deviation from symmetry in the flow field is probably caused by the assymmetry of the mesh.

  However, the chart with the mass balance deviations denoted (Figure 18) indicates that the deviation index in this case is in fact in generally a little bit higher than that for Case 3.

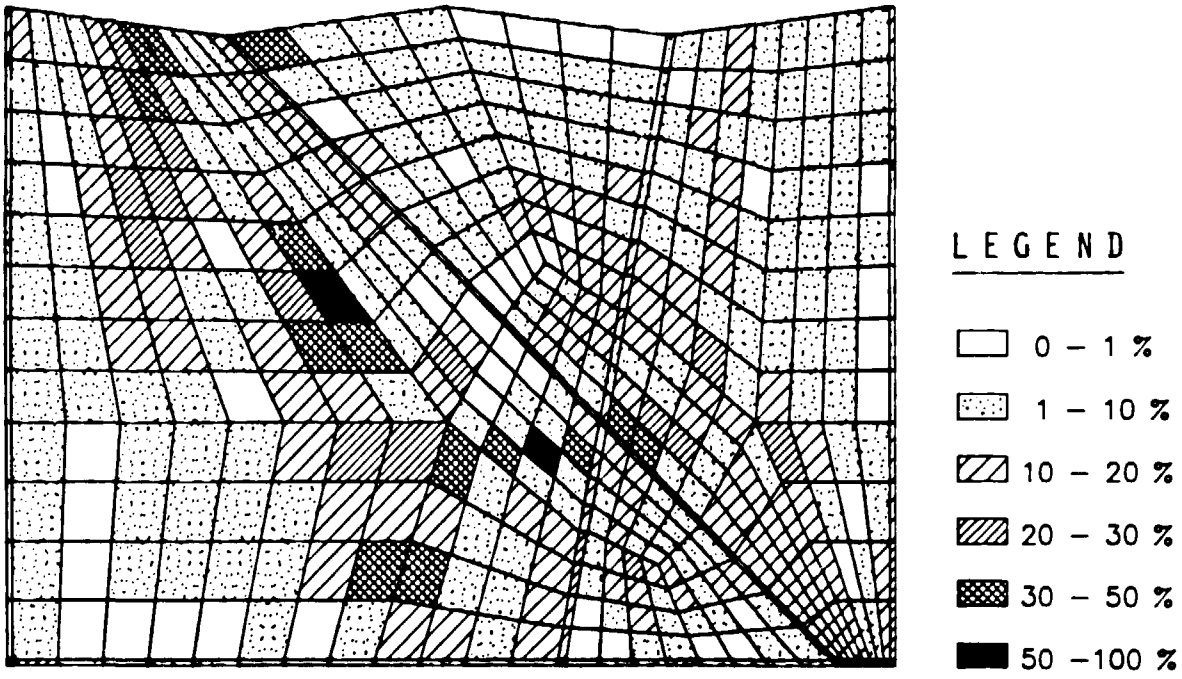

Fig. 18 Mass balance deviation index in Case 4.

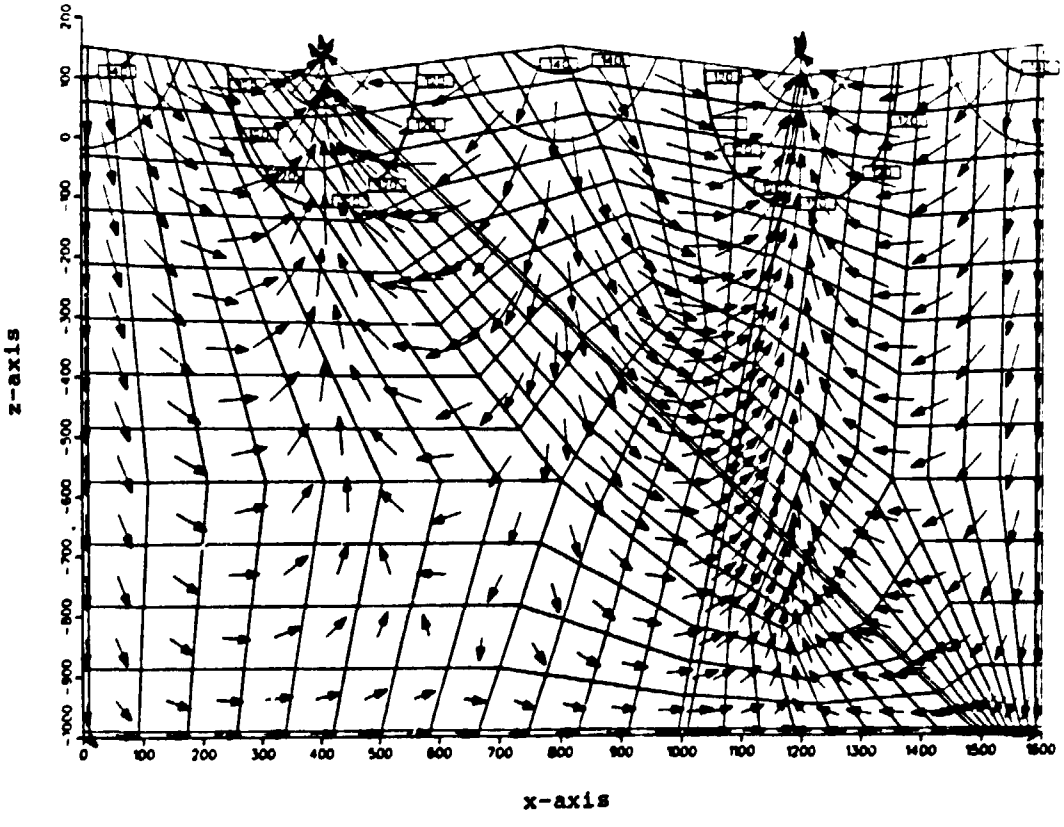

Fig. 19 Isopotentials and flow vectors in Case 4.

- Contrast in hydraulic conductivity of 10 times, Case 5.

  A contrast in hydraulic conductivity of 10 times is here assigned by keeping the conductivity of the matrix constant from Case 4 and modelling the fractures as being 10 times more pervious.

  The flow vectors and isopotential curves are shown in Figure 21. The flow is now naturally somewhat more directed towards the fractures due to their being more pervious than in Case 4. However,a significant part of the flow traverses the thinner and more slanted of the two zones.

  The mass balance deviation indices depicted in Figure 20 indicate that a somewhat numerical better solution is obtained here than in Case 4, although the differences are too small to be significant.

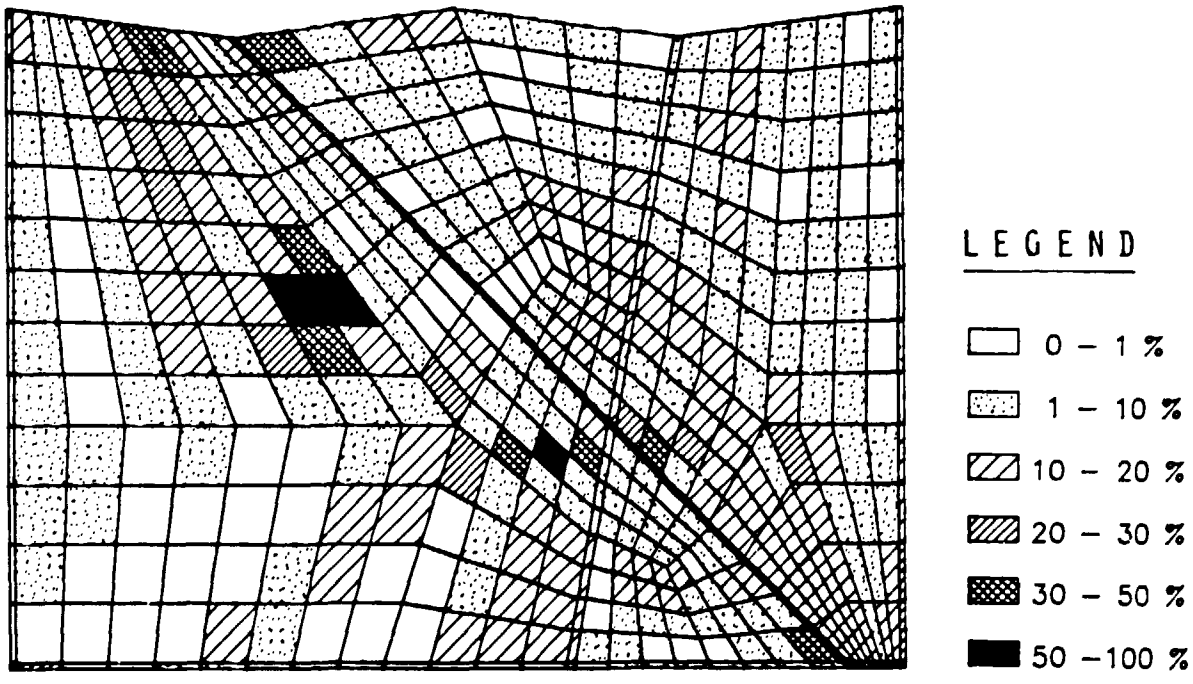

Fig. 20 Mass balance deviation index in Case 5.

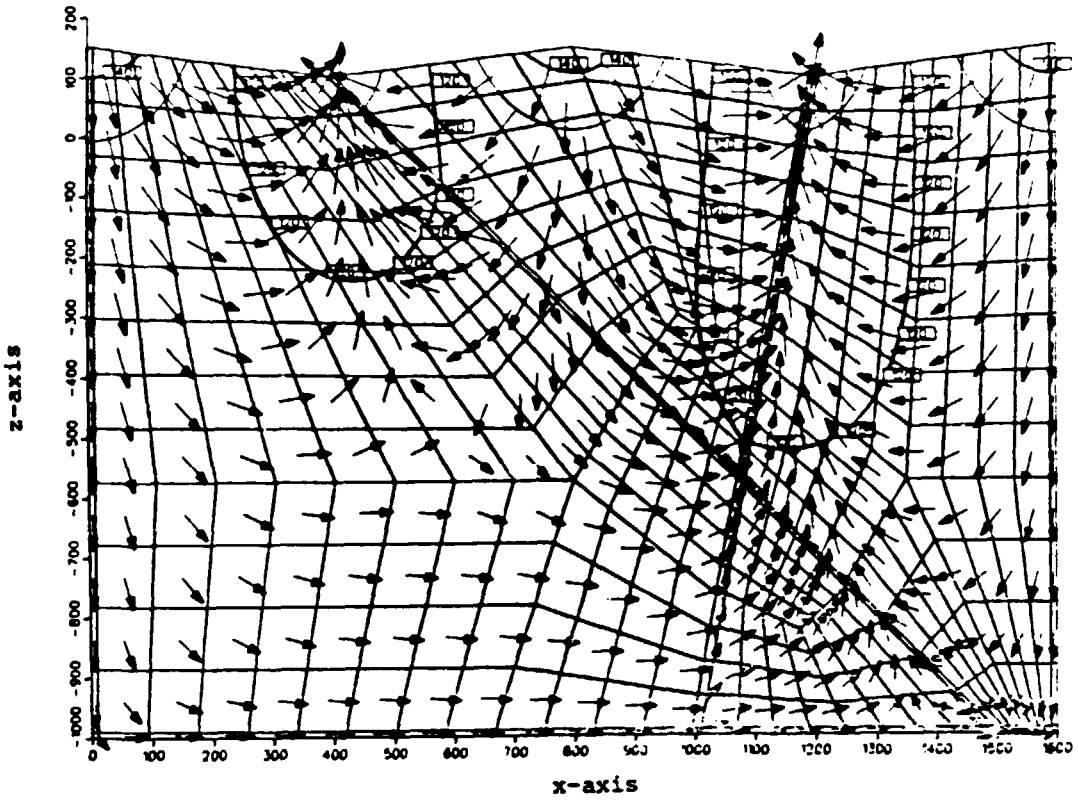

Fig. 21 Isopotentials and flow vectors in Case 5.

- Contrast in hydraulic conductivity of 1000 times, Case 6.

  The last case of this part of the study includes a contrast in hydraulic conductivity of 1000 times by keeping the conductivity of the rock mass constant and increasing it for the fractures. The effect of this high contrast is clear from analysing the plot of the isopotential curves and flow vectors, Figure 23. The flow in the rock mass is directed straight into the fracture zones more distinctly than for Case 5. This is of course a direct consequence of the increased hydraulic conductivities assigned to the fractures.

  Again, the mass balance deviation indices in this case indicate that the numerical solution has improved somewhat compared to Case 5 despite the increase in permeability contrast.The differences are,however,small (see Figure 22).

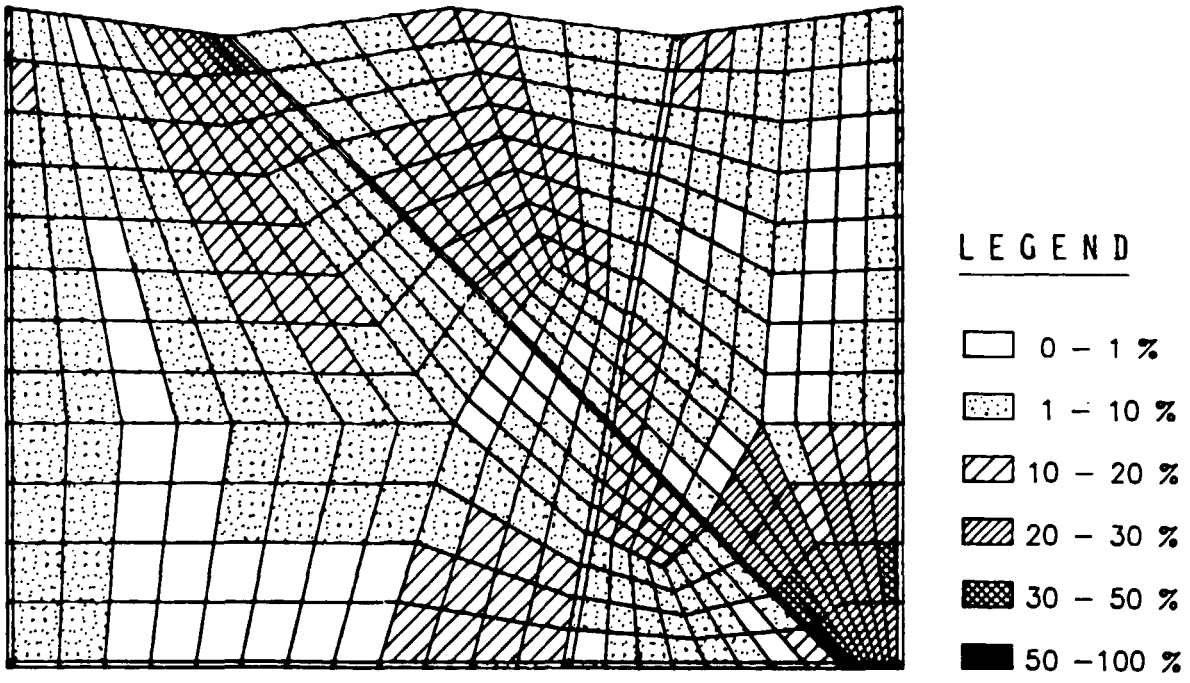

Fig. 22 Mass balance deviation index in Case 6.

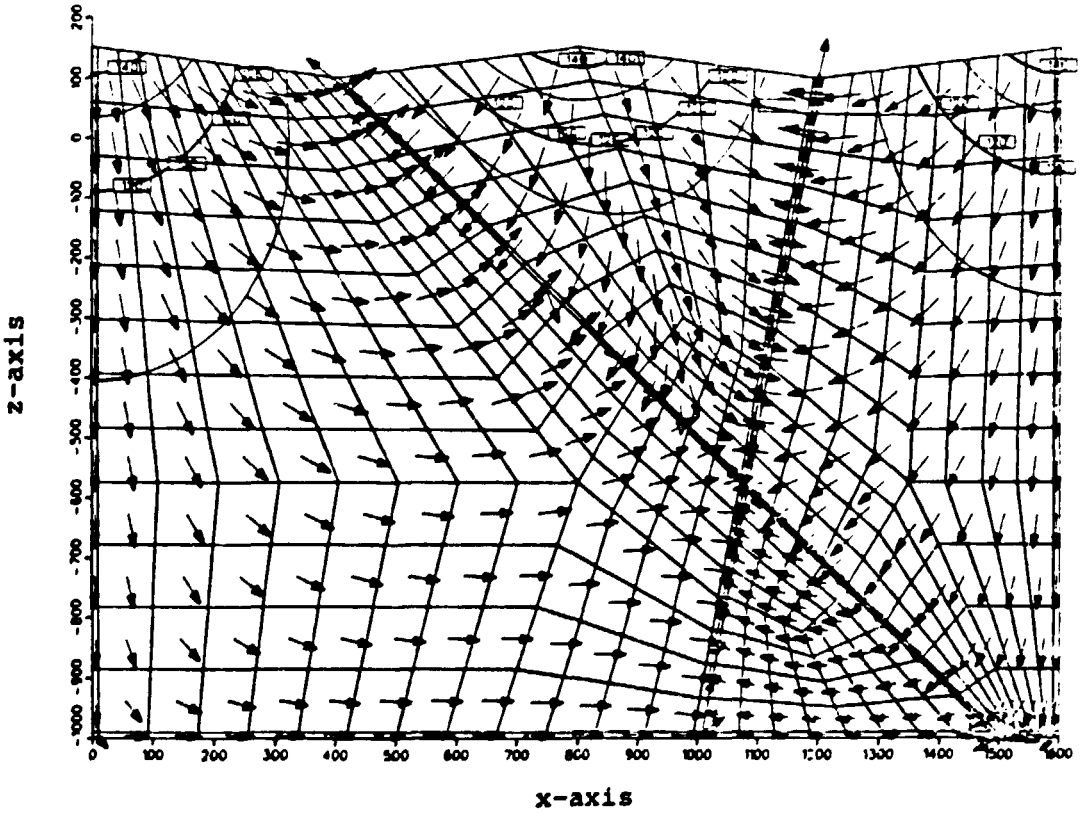

Fig. 23 Isopotentials and flow vectors in Case 6.

8.3.3 Distortion of Finite Elements (Case 7).

In order to analyse possible effects on the solution caused by distorted elements, the mesh from Case 3 is used and deformed. The results from calculations using both the original and deformed mesh are compared, and no significant difference can be seen between the two sets of results.

Hydraulic conductivities equal to those of Case 3 are assigned. The numbers of nodal points and finite elements are retained from Case 3, but the mesh is rearranged so that the shape of most of the elements is changed, compare Figures 2c and 2e (Chapter 5).

- Distorted elements, Case 7.

  The isopotential curves and flow vectors for Case 7 are shown in Figure 25.Compared to those for Case 3 (Figure 17), it turns out that the solutions are rather alike, although certain minor insignificant differences are distinguishable.

  The mass balance deviations are not exactly alike for the two cases, compare Figures 16 and 24. In certain regions of the two meshes there are some minor differences,but they are still not significant. These differences could be imaginary since many elements have changed not only in shape, but also in size.

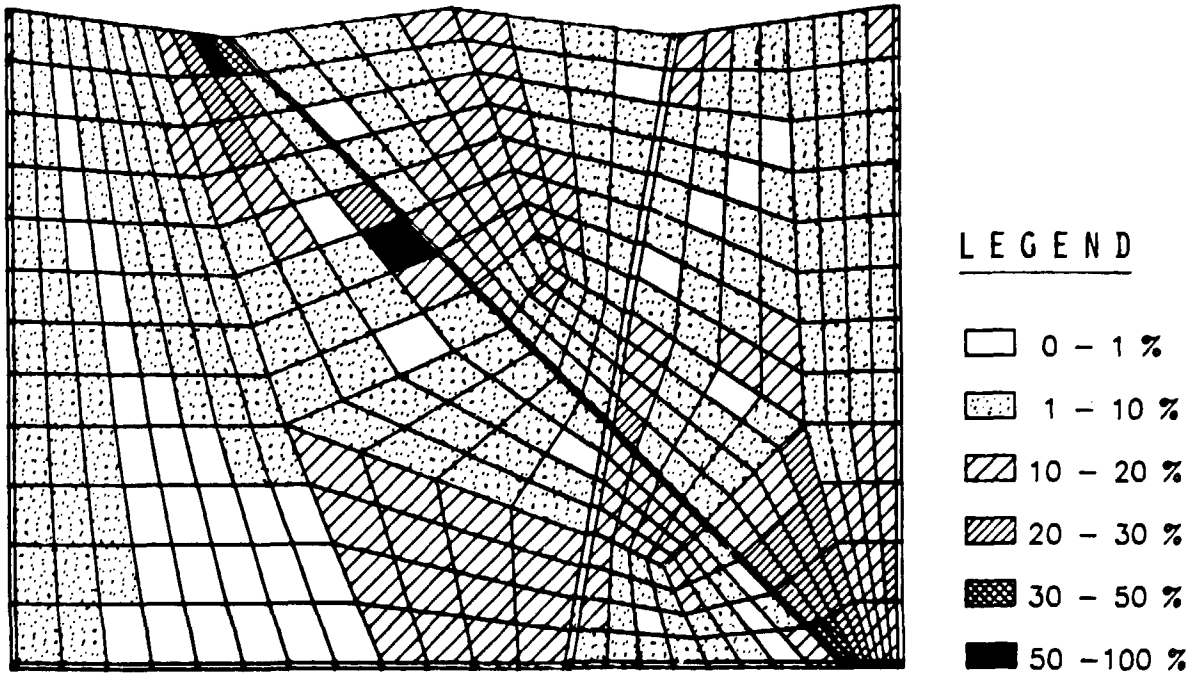

Fig. 24 Mass balance deviation index in Case 7.

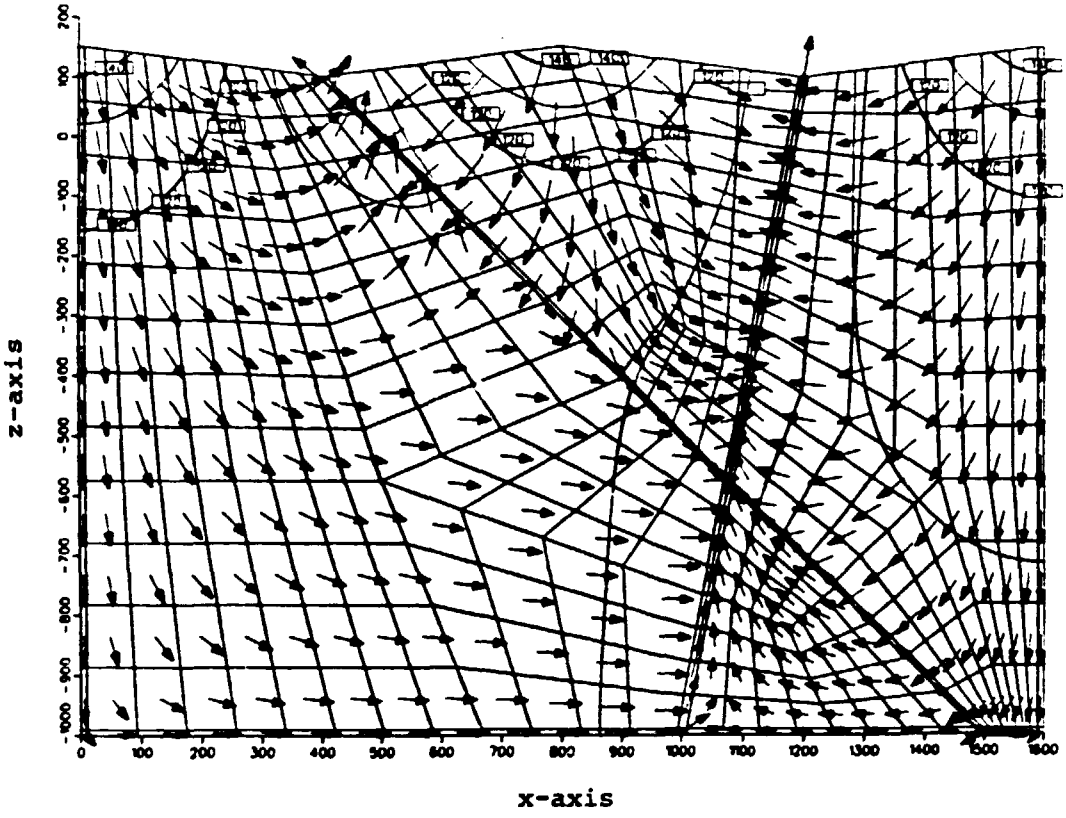

Fig. 25 Isopotentials and flow vectors in Case 7.

9 CONCLUSIONS

Concerning the head distribution within the domain it is obvious that the level of discretisation is important. A general conclusion regarding the level of discretisation is that the finest mesh gives a higher potential over the entire domain. The head distributions for the medium and fine meshes are closer to each other than corresponding values for the coarse and medium meshes.

In particular it would appear necessary to have a high enough nodal density when generating particle tracks. This is emphasized if a comparison is made for Pathline 2 calculated with the coarse and medium meshes respectively.The discretisation in the coarse mesh is too sparse; the model is not sensitive enough to detect the water divide located in the area of the turnpoint for Pathline number 2. The solutions obtained with the medium and fine meshes hardly differ at all, which indicates that obtaining an ultimate improvement in the solution could be a very expensive procedure.

Furthermore,from studying the the way mass balance deviation index is arrived at in this study ,it is obvious that the level of discretisation is of great importance for the quality of the numerical solution. High nodal density yields a low mass balance deviation. The most important outcome of the exercise with varying refinement of the finite element mesh is that there is an optimum mesh refinement beyond which further refinement does not pay.

The calculations carried out in this study give lower mass balance deviations with increasing permeability contrast, which is contrary to what was anticipated. However,the magnitude of these improvements in the numerical quality is not of the order that could be regarded as significant. The reason for this unexpected behaviour may be that the flow convergence and hence the pressure drop underneath the valleys increases when the fracture zones loose their capacity to drain the rock matrix.

Results obtained with the rearranged mesh seem to differ marginally compared to the mesh used for Case 3. The differences that might occur would appear to be more or less arbitrary and negligible. The lack of major discrepancies is probably due to an excessively modest deformation.

In conclusion, this study indicates that the geometry of the elements, in particular deviations from the ideal rectangular shape, and the hydraulic gradient seem to be of major importance to the solution quality in terms of local mass balance. In this particular case the permeability contrast is of subordinate importance.

The medium density mesh seems to be adequate for describing this domain. A further refinement has given little improvement. The discretisation in the medium mesh is of about the same level as that used in previous three-dimensional applications, see for example (5).

Preliminary comparisons with results obtained by other project teams as presented in the HYDROCOIN workshops yield the conclusion that GWHRT compares well, and can therefore be regarded as a reasonably verified code.

REFERENCES

1. THUNVIK R., BRAESTER C.,
"Hydrothermal conditions around a radioactive waste repository", KBS-TR 80-19 ,1980 .

2. GRUNDFELT B.,
"GWHRT- A finite element solution to the coupled ground water flow and heat transport problem in three dimensions - Description of HYPAC, a program package for pre-and post processing finite element",
KBS TR 83-51,1983.

3. GRUNDFELT B.,
"Proposal for a Test Problem for HYDROCOIN Level 1 Case 2-Steady State Flow in a Rock Mass Intersected by Permeable Fracture Zones",Kemakta Consultants Co.,1984

4. ANDERSSON K, GRUNDFELT B., HODGKINSON D.P., JACKSON C.P., LINDBOM B.,
"HYDROCOIN Level 1 Final Report - Verification of Groundwater Flow Models with Respect to Assessment of Radioactive Disposal", OECD/NEA, (in print).

5. CARLSSON L, WINBERG A, GRUNDFELT B,
"Model calculations of the groundwater flow at Finnsjön,Fjällveden,Gideå and Kamlunge",
KBS TR 83-45,1983.

List of SKB reports

Annual Reports

1977–78
TR 121
KBS Technical Reports 1 – 120.
Summaries. Stockholm, May 1979.

1979
TR 79–28
The KBS Annual Report 1979.
KBS Technical Reports 79-01 – 79-27.
Summaries. Stockholm, March 1980.

1980
TR 80–26
The KBS Annual Report 1980.
KBS Technical Reports 80-01 – 80-25.
Summaries. Stockholm, March 1981.

1981
TR 81–17
The KBS Annual Report 1981.
KBS Technical Reports 81-01 – 81-16.
Summaries. Stockholm, April 1982.

1982
TR 82–28
The KBS Annual Report 1982.
KBS Technical Reports 82-01 – 82-27.
Summaries. Stockholm, July 1983.

1983
TR 83–77
The KBS Annual Report 1983.
KBS Technical Reports 83-01 – 83-76
Summaries. Stockholm, June 1984.

1984
TR 85–01
Annual Research and Development Report 1984
Including Summaries of Technical Reports Issued during 1984. (Technical Reports 84-01– 84-19)
Stockholm June 1985.

1985
TR 85-20
Annual Research and Development Report 1985
Including Summaries of Technical Reports Issued during 1985. (Technical Reports 85-01-85-19)
Stockholm May 1986.

Technical Reports

1986

TR 86-01
I: An analogue validation study of natural radionuclide migration in crystalline rock using uranium-series disequilibrium studies
II: A comparison of neutron activation and alpha spectroscopy analyses of thorium in crystalline rocks
J A T Smellie, Swedish Geological Co, A B MacKenzie and R D Scott, Scottish Universities Research Reactor Centre
February 1986

TR 86-02
Formation and transport of americium pseudocolloids in aqueous systems
U Olofsson
Chalmers University of Technology, Gothenburg, Sweden
B Allard
University of Linköping, Sweden
March 26, 1986

TR 86-03
Redox chemistry of deep groundwaters in Sweden
D Kirk Nordstrom
US Geological Survey, Menlo Park, USA
Ignasi Puigdomenech
Royal Institute of Technology, Stockholm, Sweden
April 1, 1986

TR 86-04
Hydrogen production in alpha-irradiated bentonite
Trygve Eriksen
Royal Institute of Technology, Stockholm, Sweden
Hilbert Christensen
Studsvik Energiteknik AB, Nyköping, Sweden
Erling Bjergbakke
Risö National Laboratory, Roskilde, Denmark
March 1986

TR 86-05
Preliminary investigations of fracture zones in the Brändan area, Finnsjön study site
Kaj Ahlbom, Peter Andersson, Lennart Ekman, Erik Gustafsson, John Smellie,
Swedish Geological Co, Uppsala
Eva-Lena Tullborg, Swedish Geological Co, Göteborg
February 1986

TR 86-06
Geological and tectonic description of the Klipperås study site
Andrzej Olkiewicz
Vladislav Stejskal
Swedish Geological Company
Uppsala, October, 1986

TR 86-07
Geophysical investigations at the Klipperås study site
Stefan Sehlstedt
Leif Stenberg
Swedish Geological Company
Luleå, July 1986

TR 86-08
Hydrogeological investigations at the Klipperås study site
Bengt Gentzschein
Swedish Geological Company
Uppsala, June 1986

TR 86-09
Geophysical laboratory investigations on core samples from the Klipperås study site
Leif Stenberg
Swedish Geological Company
Luleå, July 1986

TR 86-10
Fissure fillings from the Klipperås study site
Eva-Lena Tullborg
Swedish Geological Company
Göteborg, June 1986

TR 86-11
Hydraulic fracturing rock stress measurements in borehole Gi-1, Gideå Study Site, Sweden
Bjarni Bjarnason and Ove Stephansson
Division of Rock Mechanics,
Luleå University of Technology, Sweden
April 1986

TR 86-12
PLAN 86— Costs for management of the radioactive waste from nuclear power production
Swedish Nuclear Fuel and Waste Management Co
June 1986

TR 86-13
Radionuclide transport in fast channels in crystalline rock
Anders Rasmuson, Ivars Neretnieks
Department of Chemical Engineering
Royal Institute of Technology, Stockholm
March 1985

TR 86-14
Migration of fission products and actinides in compacted bentonite
Börje Torstenfelt
Department of Neclear Chemistry, Chalmers University of Technology, Göteborg
Bert Allard
Department of water in environment and society, Linköping university, Linköping
April 24, 1986

TR 86-15
Biosphere data base revision
Ulla Bergström, Karin Andersson, Björn Sundblad, Studsvik Energiteknik AB, Nyköping
December 1985

TR 86-16
Site investigation
Equipment for geological, geophysical, hydrogeological and hydrochemical characterization
Karl-Erik Almén, SKB, Stockholm
Olle Andersson, IPA-Konsult AB, Oskarshamn
Bengt Fridh, Bengt-Erik Johansson,
Mikael Sehlstedt, Swedish Geological Co, Malå
Erik Gustafsson, Kenth Hansson, Olle Olsson,
Swedish Geological Co, Uppsala
Göran Nilsson, Swedish Geological Co, Luleå
Karin Axelsen, Peter Wikberg, Royal Institute of Technology, Stocholm
November 1986

TR 86-17
Analysis of groundwater from deep boreholes in Klipperås
Sif Laurent
IVL, Swedish Environmental Research Institute
Stockholm, 1986-09-22

TR 86-18
Technology and costs for decommissioning the Swedish nuclear power plants.
Swedish Nuclear Fuel and Waste Management Co
May 1986

TR 86-19

Correlation between tectonic lineaments and permeability values of crystalline bedrock in the Gideå area

Lars O Ericsson, Bo Ronge
VIAK AB, Vällingby
November 1986

TR 86-20

A Preliminary Structural Analysis of the Pattern of Post-Glacial Faults in Northern Sweden

Christopher Talbot, Uppsala University
October 1986

ISSN 0348-7504